Many-Body Quantum Chaos and Emergence of Ginibre Ensemble

Saumya Shivam, Andrea De Luca, David A. Huse, and Amos Chan

Phys. Rev. Lett. **130**, 140403 — Published 7 April 2023

DOI: 10.1103/PhysRevLett.130.140403

Many-body quantum chaos and emergence of Ginibre ensemble

Saumya Shivam,[1] Andrea De Luca,[2] David A. Huse,[1] and Amos Chan[3]

[1] *Department of Physics, Princeton University, Princeton, New Jersey 08544, USA*

[2] *Laboratoire de Physique Théorique et Modélisation, CY Cergy Paris Université, CNRS, F-95302 Cergy-Pontoise, France*

[3] *Princeton Center for Theoretical Science, Princeton University, Princeton NJ 08544, USA*

(Dated: March 7, 2023)

We show that non-Hermitian Ginibre random matrix behaviors emerge in spatially-extended many-body quantum chaotic systems in the space direction, just as Hermitian random matrix behaviors emerge in chaotic systems in the time direction. Starting with translational invariant models, which can be associated with dual transfer matrices with complex-valued spectra, we show that the linear ramp of the spectral form factor necessitates that the dual spectra have non-trivial correlations, which in fact fall under the universality class of the Ginibre ensemble, demonstrated by computing the level spacing distribution and the dissipative spectral form factor. As a result of this connection, the exact spectral form factor for the Ginibre ensemble can be used to universally describe the spectral form factor for translational invariant many-body quantum chaotic systems in the scaling limit where t and L are large, while the ratio between L and L_{Th}, the many-body Thouless length is fixed. With appropriate variations of Ginibre models, we analytically demonstrate that our claim generalizes to models without translational invariance as well. The emergence of the Ginibre ensemble is a genuine consequence of the strongly interacting and spatially extended nature of the quantum chaotic systems we consider, unlike the traditional emergence of Hermitian random matrix ensembles.

Introduction.– The discovery of the connection between quantum chaos and random matrix theory (RMT) is of great importance in theoretical physics because RMT provides an approach that eliminates dependence on the microscopic details and captures the universal characteristics of an ensemble of statistically similar chaotic systems, constrained only by symmetries [1, 2]. Historically, the spectral correlation of the Gaussian ensembles was discovered in chaotic mesoscopic systems for sufficiently small energy scales or equivalently, sufficiently late time scales [3, 4]. Recently, with the development in random unitary circuits [5–18], particularly in the time periodic or Floquet circuits, Recent analytic calculations of random matrix behaviour in spectral correlations of spatially-extended *many-body* quantum chaotic systems been achieved [19–27]. While Floquet circuits have given access to the study of non-trivial spectral properties in extended many-body systems — like the onset of RMT behaviour [20, 25, 27–29], spectral Lyapunov exponents [26], and novel scaling forms and limits [23, 25] — translational-invariant (TI) circuits give rise, via the so-called space-time duality, to non-Hermitian dual transfer matrix (Fig. 1 red) with complex eigenvalues, the dual spectrum. The study of many-body quantum system using space-time duality began in the study of the kicked Ising model at the self-dual point [22, 30–33] and concurrently in the transfer matrix approach in Floquet circuits [20, 25, 26]. Subsequently, numerous works have investigated the non-unitary "dynamics" in the space direction [34–38]. The objective of this paper is to provide evidence of the emergence of non-Hermitian Ginibre (GinUE) RMT-behaviour [39] in many-body quantum chaotic (MBQC) systems in the thermodynamic and scaling limit, in contrast to the emergence of standard Gaussian Hermitian RMT ensembles in late time, as illustrated below.

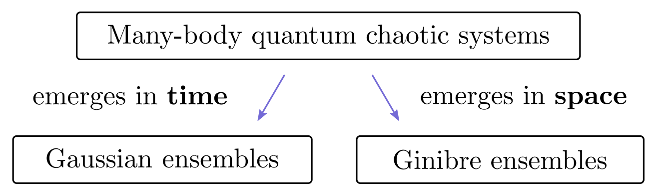

Heuristics.– One of the simplest non-trivial and analytically-tractable quantities to diagnose chaos is the *spectral form factor* (SFF), defined as [2, 19–23, 25–29, 31, 41–55]

$$K(t,L) = \left\langle \left|\mathrm{Tr}_{\mathcal{H}}\left[\mathcal{W}(t,L)\right]\right|^2 \right\rangle = \left\langle \left|\mathrm{Tr}_{\tilde{\mathcal{H}}}\left[\mathcal{V}(t,L)\right]\right|^2 \right\rangle \quad (1)$$

where $\mathcal{W}(t,L) = \prod_{t'=1}^{t} W(t',L)$ is a time evolution operator acting on Hilbert space $\mathcal{H}$, and $\mathcal{V}(t,L) = \prod_{j=1}^{L} V(t,j)$ is the corresponding dual operator (Fig. 1 red) performing "evolution" in space on dual Hilbert space $\tilde{\mathcal{H}}$. t and L denote the numbers of repeated actions of W and V, and can be treated as effective time and system size respectively [56] . For Floquet systems, one has $W(t',L) = W(L)$, while $V(t,j) = V(t)$ for TI systems with transfer matrix $V(t)$. We can generally diagonalise $V(t)$ with the eigenvalues $\{z_j\} \equiv \{\rho_j e^{\imath\phi_j}\}$ with $\rho_j, \phi_j \in \mathbb{R}$.

$$K(t,L) = \left\langle \sum_i \rho_i^{2L} + \sum_{i\neq j}\left[e^{i(\phi_i-\phi_j)}\rho_i\rho_j\right]^L \right\rangle \quad (2)$$

We are denoting as $\langle \ldots \rangle$ the ensemble average over statistically similar systems. In the absence of extra sym-

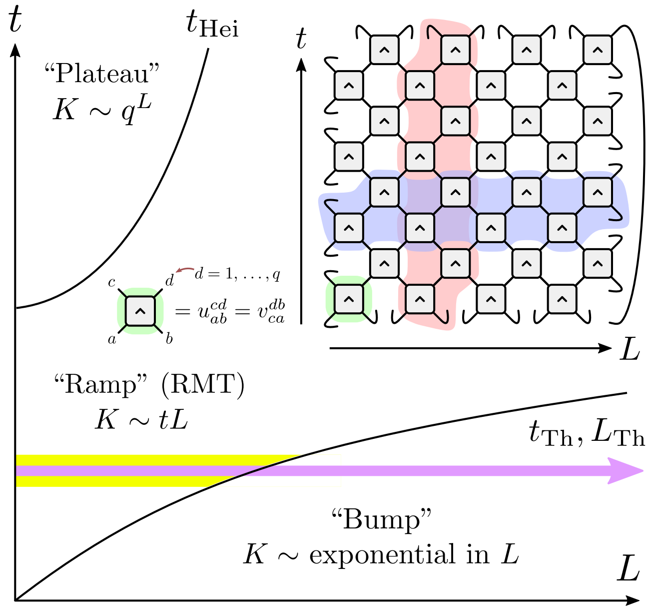

FIG. 1. Regime diagram of spectral form factor $K(t, L)$ (Eq 1) for many body quantum chaotic systems with translational invariance in space and time, with ‘Bump’, random matrix ‘Ramp’ (RMT) and ‘Plateau’ regimes. For fixed t and increasing L (purple), the SFF exhibits an initial linear ramp behavior (yellow) which necessarily requires non-trivial spectral statistics of the dual spectra. Inset: Diagrammatical representation of equality of the spectral form factor computed using the dual transfer matrix (Eq 1) , with unitary 2-gate (green), Floquet operator $W(L)$ (blue), dual transfer matrix $V(t)$ (red).

metries, RMT predicts $K(t, L) \sim tL$ for TI Floquet systems. This can be understood as the spectrum of $W(L)$ splits in L momentum sectors which emerges because of TI. If correlations between sectors vanish, the spectral form factor results from the sum of the usual linear-in-t behavior within each momentum sector [23]. For many-body systems, this RMT behavior emerges whenever $t > t_{\text{Th}}(L)$ or equivalently $L < L_{\text{Th}}(t)$, where $t_{\text{Th}}(t)$, $L_{\text{Th}}(L)$ are respectively the many-body SFF Thouless time and length, related by $L_{\text{Th}}(t_{\text{Th}}(L)) = L$. The Thouless time is a system-dependent quantity which characterises the time scale for the onset of chaos in the two-point level correlation and in general is expected to grow with system size L [23] (with the relevant exception of the dual–unitary circuits [22, 31, 36, 41, 57–59]). It is insightful to re-interpret these considerations in terms of the spectrum of $V(t)$. From Eq. (2), we see that if phase correlations could be neglected, $K(t, L) \gtrsim e^{\lambda(t)L}$, with $\lambda(t) = \max_i \ln \rho_i$ for $L \gg L_{\text{Th}}(t)$. We label this regime as the “Exponential bump” region in Fig. 1. Thus, the existence of the “Ramp” regime, characteristic of RMT, for $L \lesssim L_{\text{Th}}(t)$ implies that the off-diagonal term in (2) *necessarily* display non-trivial correlation, such that the exponential behaviour of the diagonal term in (2) could be compensated. We emphasize that this heuristic argument applies to generic translational invariant MBQC systems. The characterisation of the spectral statistics of $V(t)$ will be the main objective of this letter. As we show below, such dual spectral statistics falls under the universality class of Ginibre ensemble, which can be seen as the most generic rotation invariant Gaussian ensemble, once all relevant symmetries have been taken into account (e.g. space-time translational invariance).

Models. – We consider three one-dimensional random unitary circuits as models of MBQC, namely the brick-wall model, the random phase model, and the kicked Ising model. All three models can be written as the operator $\mathcal{W}(t, L) = \prod_{t'=1}^{t} W(t', L) = \prod_{r=1}^{L} V(t, r) = \mathcal{V}(t, L)$ where $W(t', L)$ and $V(t, r)$ refer respectively to the time and space transfer matrix shown in blue and red in Fig. 1, acting on the Hilbert space with dimensions q^L and q^t respectively, with q being the on-site dimension [56]. The circuit is composed of unitary two-gates $u(t', r)$ and one can define the space-time dual of u via $u^{cd}_{ab}(t', r) = v^{db}_{ca}(t', r)$. The precise definitions of the gates $u(t', r)$ are given in the supplementary material [40], and are not crucial for our discussion as long as the models are chaotic and have no conserved quantities. We define four setups resulting from the combination of translational invariance in space and time: (a) Temporally and spatially random unitary circuits, where all u-s are drawn independently. In this case, spectral correlations are trivial in both space and time directions, with $K(t, L) \sim 1$ for all t, L [23]; (b) Temporally periodic, i.e. Floquet, and spatially random (Floquet) circuits, where $u(t', r) = u(t'', r)$ for all t', t'' and r; (c) Temporally random and spatially TI random circuits, where $u(t', r) = u(t', r')$ for all t', r and r'; and (d) Floquet and spatially TI (TIF) circuits, where $u(t', r) = u(t'', r')$ for all t', t'', r and r'.

Dual spectral statistics.– We start by focusing on TI (temporal random) models (case c), where the transfer matrix $V(t)$ has a well-defined spectrum and exhibits no additional symmetries since the model is temporarily disordered. As the spectrum is complex, in order to analyse its correlations, we resort to a) level spacing distribution and b) a natural generalization of SFF, known as the *dissipative spectral form factor* [47]. The SFF of a generic complex spectrum is exponentially growing or decaying due to the imaginary parts of the complex eigenvalues. To circumvent this problem, dissipative SFF instead treats the complex spectrum as a set of points in the plane and assess the distribution of their euclidean distances. Indeed, for a non-Hermitian operator with spectrum $\{z_n = x_n + iy_n : x_n, y_n \in \mathbb{R}\}$, the connected part is defined as

$$\mathcal{K}_c(t, s) := \left\langle \left| \sum_n e^{ix_n t + iy_n s} \right|^2 \right\rangle - \left| \left\langle \sum_n e^{ix_n t + iy_n s} \right\rangle \right|^2, \qquad (3)$$

where t and s are two generalized time variables. We organise them into the complex time $\tau \equiv t + is \equiv |\tau| e^{\imath\theta}$,

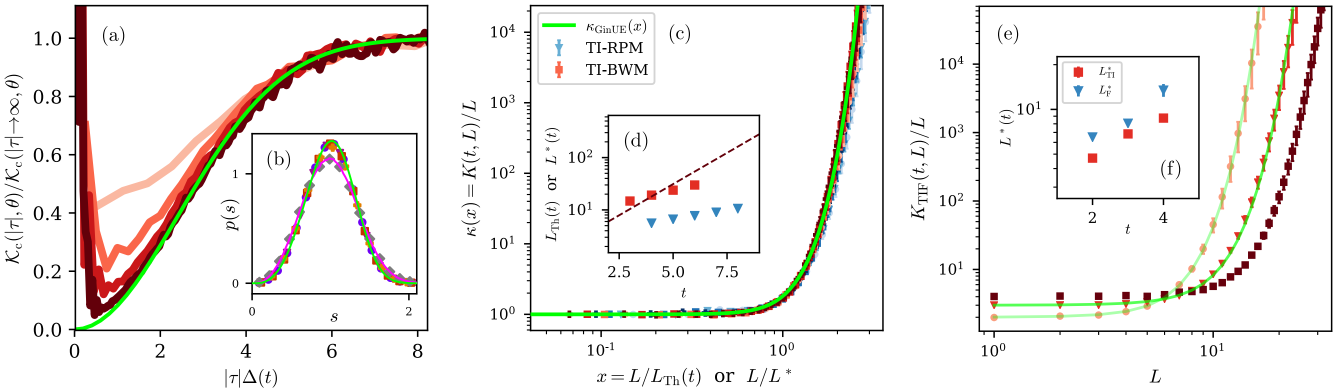

FIG. 2. Universal correlations for representative many body random quantum circuits [40], showing approach to corresponding quantities computed for the Ginibre ensemble (green). (a): Dissipative spectral formm factor (3) of the dual spectra of the brick wall model, for $t = 3, 4, 5, 6$ from light to dark red. (b): Nearest neighbour spacing distribution of the dual spectra of the brick wall model (on site dimension $q = 2, t = 6$, purple), random phase model ($q = 3, t = 8$, burgundy), and zero momentum sectors of translational invariant Floquet brick wall model ($q = 2, t = 7$, red) and random phase model ($q = 3, t = 10$, gold). Kicked Ising model away from the self dual point at $J = 0.75J_c$ (grey) shows the distribution corresponding to the symmetric Ginibre ensemble (pink curve obtained from $N = 2187$) due to time reversal symmetry [40]. (c): Scaling collapse of the spectral form factor $\kappa_{\rm TI}(x)$ for two models and $\kappa_{\rm Gin}(x)$, for the Ginibre ensemble (8), against $x = L/L_{\rm Th}$ or L/L^* with excellent agreement, where $L_{\rm Th}$ is Thouless length, and L^* is the inverse mean level spacing for Ginibre ensemble. (d): $L/L_{\rm Th}$ (dots) and L^* (dashed line) against time t, used for the collapse in the main panel. For Ginibre, we define an effective time via $N := q^t$. (e): Scaled spectral form factor $K_{\rm TIF}(t, L)/L$ for translational invariant Floquet brick wall model ($q = 3, t = 2, 3, 4$, red) and the numerical fit of $K_{\rm TIF-Gin}(t, L)/L$ (green) against L with darker colors for larger t. We fit $K_{\rm TIF-Gin}(t, L)$ to $K_{\rm TIF}(t, L)$ by tuning $L^*_{\rm F}$ and $L^*_{\rm TI}$ in Eq. (12), which are plotted against time t as blue and red respectively in (f).

and will abusively use the polar coordinate $(|\tau|, \theta)$ to parameterise the arguments of $\mathcal{K}_c$. As a yardstick for the generic behavior of $\mathcal{K}_c$, we consider the GinUE, sampled by taking N-by-N random matrices with independent complex Gaussian matrix element with variance $\sigma^2 = v/N$. In other words, the probability density for a matrix M is $\propto \exp[-N/(2v)\,{\rm Tr}\, MM^\dagger]$, and is thus rotational invariant. Therefore, the GinUE is expected to capture the spectral correlations of sufficiently generic, or "chaotic", complex non-Hermitian matrices, in a similar fashion to how the Gaussian and Circular unitary ensemble are the universality class for unitary and hermitian matrices respectively [47, 60]. The dissipative SFF can be computed explicitly for GinUE [47]. Keeping the leading contribution in N, $\mathcal{K}_c$ simplifies to

$$\mathcal{K}_{\rm c,Gin}(|\tau|, \theta) = \frac{N}{v}\left(1 - e^{-\frac{v|\tau|^2}{4N}}\right). \tag{4}$$

which is rotational symmetric and shows a *(dip-)ramp-plateau* behaviour [61], analogous to the SFF for closed quantum systems: At $|\tau| \lesssim \Delta^{-1} \sim \sqrt{N}$, it increases *quadratically* $\simeq |\tau|^2/4$ in large N until it plateaus at N at a time comparable to the inverse of the mean level spacing Δ in the complex plane. Remarkably, the quadratic ramp of dissipative SFF for GinUE is drastically different from the corresponding behaviour for Gaussian unitary ensembles, which is *linear* in time. The quadratic ramp is sensitive to the variation of density of states across the complex plane, and thus unfolding is required to uncover the true long-range dual spectral correlations [40]. In Fig. 2a, we show for TI random phase model, as a representative example, a good collapse of $\mathcal{K}_c(|\tau|, \theta)/\mathcal{K}_c(|\tau| \to \infty, \theta)$ against $|\tau|\Delta$, approaching GinUE behaviour (4) as the dual system size t increases, with a similar approach for other models [40], demonstrating universality.

To provide further evidence of emergence of GinUE, we probe the spectral correlation at the scale of mean level spacing in the complex plane using the nearest-neighbour spacing distribution in Fig. 2b, and complex spacing ratio [62] in [40], for the three different TI models. We find signatures of level repulsion consistent with the corresponding RMT universality classes (including the ones with time reversal symmetry [40]), and with the dissipative SFF results around the Δ^{-1} region.

SFF of GinUE.– With the insight that dual-spectral correlation falls under the universality class of GinUE, it is natural to ask whether this information can be used to understand the behavior of the SFF. As before, we start by focusing on TI systems, where, in the absence of extra symmetries, the correlation of the dual spectrum are captured by the standard GinUE, whose joint probability distribution function of eigenvalues $\{z_j\}$ is known exactly [63]. We model the SFF in (1), by replacing the transfer matrix $V(t)$ with $V_{\rm G}$ drawn from the GinUE of size N, and obtain [40]

$$K_{\text{Gin}}(N,L) := \left\langle \left|\text{Tr}\left[V_{\text{G}}^{L}\right]\right|^{2}\right\rangle$$
$$= N^{2}\delta_{L,0} + \frac{v^{L}\left((L+N)! - \frac{N!(N-1)!}{(N-L-1)!}\right)}{N^{L}(L+1)(N-1)!} \ . \tag{5}$$

In matching the predictions of (5) with many-body models, we encode t dependence in the matrix size N, whose functional form will be specified later. In the limit of large N at fixed large L, $K_{\text{Gin}}(N,L) = v^{L}L(1 + O(L^{4}/N^{2}))$. The crossover scale $L^{*}_{\text{TI}} = \sqrt{N}$ is related to the inverse of mean level spacing Δ in the complex plane. This suggests a scaling limit where L and N are sent to infinity with $x = L/L^{*}_{\text{TI}}$ fixed and one has

$$\kappa_{\text{Gin}}(x) \equiv \lim_{\substack{L,N\to\infty \\ x=L/L^{*}_{\text{TI}}}} \frac{K_{\text{Gin}}}{v^{L}L} = \frac{2\sinh\left(\frac{x^{2}}{2}\right)}{x^{2}} \ . \tag{6}$$

In fact, the above scaling form of GinUE shares similarities with the scaling forms proposed for TI (temporal random) systems in [23], given by

$$\kappa_{\text{TI}-\text{MBQC}}(x) = \lim_{\substack{L,t\to\infty \\ x=L/L_{\text{Th}}(t)}} \frac{K_{\text{TI}-\text{MBQC}}}{L} \ , \tag{7}$$

for TI systems, where instead of L^{*}_{TI} in GinUE, the system-dependent many-body Thouless length $L_{\text{Th}}(t)$ is used to define the scaling limit. Now, given that (i) the spectral correlation dual spectra of many body chaotic systems falls under the GinUE universality class; (ii) a linear ramp in L naturally emerges from (5) for $L \ll L^{*}_{\text{TI}}$, coinciding with the appearance of the linear-ramp in SFF of chaotic systems; we conjecture that the scaling form of GinUE describes the scaling form of TI chaotic systems once L^{*}_{TI} and $L_{\text{Th}}(t)$ are identified, i.e.

$$\kappa_{\text{TI}-\text{MBQC}}(x) = \kappa_{\text{Gin}}(x) \equiv \kappa_{\text{TI}-\text{Gin}}(x) \ , \tag{8}$$

To test this claim, we simulate both sides of (8), for TI brick wall model, random phase model, and GinUE in Fig. 2c and find an excellent collapse. We note that the scaling limit in (7) differs from the infinite-q result obtained for the random phase model in [23] which disagreed with the finite-q numerical simulations. The universality of $\kappa(x)$ implies that the microscopic details are only reflected in the function $L_{\text{Th}}(t)$, and not in the scaled function $\kappa(x)$, as observed in [23]. Also, the validity of Eq. (8) indicates that the effective size N of the equivalent GinUE matrix shall not be fixed from the dual Hilbert space dimension ($= q^{2t}$), but rather from the emerging Thouless length, i.e. $N = L^{*2} \sim L_{\text{Th}}(t)^{2} \ll q^{2t}$ (Fig. 2d).

Beyond translational invariance.– We now extend the previous considerations to Floquet systems. We first consider with spatial randomness (case b) and then we incorporate TI (case d), and demonstrate the emergence of GinUE–like behaviour with and without TI. To incorporate time periodicity, we first observe that the transfer matrix becomes invariant under time translations, and thus its spectrum can be split in *time momentum* or frequency sectors. In the inset of Fig. 2b and [40], we respectively compute the dissipative SFF and spacing distribution for the dual spectrum in each sector, and confirm the emergence of Ginibre statistics. Time translation implies $V(t,r) = TV(t,r)T^{-1}$, where T shifts the dual system over one period. For simplicity, we assume invariance under one site translation, with $T\left|\mathbf{s} = s_{1}s_{2}\dots s_{t}\right\rangle = \left|s_{2}s_{3}\dots s_{t}s_{1}\right\rangle$, generalization to longer unit cells being straightforward. For each configuration $\mathbf{s}$, we define its associated *period* as the minimal $\tau = 1,\dots,t$ such that $T^{\tau}\left|\mathbf{s}\right\rangle = \left|\mathbf{s}\right\rangle$. To formulate the statistical properties of the ensemble, we restrict the Hilbert space to the set of computational basis $\{\left|\mathbf{s}\right\rangle\}$ translational invariant with only period t. Indeed, the fraction of configurations with maximal period goes to 1 for large t (and/or obviously for large q). Using N_{o} to denote the number of distinct orbits under the translation operation, we formally have a dimension for the restricted dual Hilbert space $\dim(\tilde{\mathcal{H}}) = tN_{\text{o}}$. Then, we model the transfer matrix $V(t,r)$ by a random matrix V_{G} with complex Gaussian entries and covariance

$$\left\langle [V_{\text{G}}]_{\mathbf{ss}'}[V_{\text{G}}]^{*}_{\mathbf{pp}'}\right\rangle = \frac{1}{N_{\text{o}}}\sum_{\tau,\tau'}\delta_{\mathbf{s}T^{\tau}(\mathbf{p})}\delta_{\mathbf{s}'T^{\tau'}(\mathbf{p}')}J(\tau-\tau') \ , \tag{9}$$

where $J(\tau-\tau')$ controls the correlation between matrix elements. As pointed out in [64] via a semiclassical expansion, the emergence of SFF linear ramp using RMT $K(t) = t$ in single-particle chaotic Floquet systems can be associated to the pairing between two periodic orbits, which can happen in t possible ways (t being the discrete length of the orbit here). In extended chaotic systems, the factor of t corresponds to the possible values of $\tau = 1,\dots,t$ for *local* pairing of orbits [20, 45]. The interaction between neighbouring local degrees of freedom forces similar pairings between local orbits, quantified here by the function $J(\tau-\tau')$. A simple calculation gives $K_{\text{F}-\text{Gin}}(t,L) = \left\langle \left|\text{Tr}[V_{\text{G}}(t,L)]\right|^{2}\right\rangle = \sum_{\{\tau\}}\prod_{i=1}^{L}J(\tau_{i}-\tau_{i+1}) = \sum_{\omega}[\hat{J}(\omega)]^{L}$ [40], with $\hat{J}(\omega)$ the Fourier transform of $J(\tau)$. We thus see that the SFF behavior in the scaling limit depends on $\hat{J}(\omega)$. For simplicity, we suppose $J(\tau-\tau') = \delta_{\tau,\tau'} + f(t)h(\tau-\tau')$, where $f(t)$ decays to zero on the scale of the Thouless time, and the function $h(\tau-\tau')$ controls the correlation between neighbouring pairings. Within this formulation, the scaling limit depend on the details of the Fourier transform $\hat{h}(\omega)$. However, the exact calculation in the random phase model at infinite q [20, 23, 40] leads to $h(\tau-\tau') = 1 - \delta_{\tau,\tau'}$ which implies $\hat{h}(\omega) = t\delta_{\omega,0} - 1$. Numerical evidence supports the claim that in general $\hat{h}(\omega \neq 0)/\hat{h}(\omega = 0) \overset{t\to\infty}{\to} 0$. Under this assumption, one recovers the emergent *Potts model* of SFF [40] and the universal result from [20, 23],

$$\kappa_{\mathrm{F-Gin}}(x) = \lim_{\substack{L,t\to\infty \\ x=L/L_{\mathrm{F}}^*(t)}} K_{\mathrm{F-Gin}} - t = e^x - x - 1\ , \quad (10)$$

with $L_{\mathrm{F}}^*(t) = [f(t)\hat{h}(0)]^{-1}$. Hence, we have for case b

$$\kappa_{\mathrm{F-Gin}}(x) = \kappa_{\mathrm{F-MBQC}}(x)\ . \quad (11)$$

Translation invariant Floquet case. – For TI Floquet systems (case d), we model the transfer matrix with (9), except that TI is imposed, i.e. $V_{\mathrm{G}}(t,r) = V_{\mathrm{G}}(t,r')$ for all r, r'. In practice, Eq. (9) implies that different frequency sectors are statistically decoupled. We can thus evaluate $K_{\mathrm{TIF-Gin}}$ for this model, using Eq. (5) within each sector and replacing the variance $v/N \to \hat{J}(\omega)/N_{\mathrm{o}}$. Using the results in Eqs. (6,10), one obtains for $L \neq 0$,

$$\begin{aligned} K_{\mathrm{TIF-Gin}}(t,L) &= K_{\mathrm{Gin}}(N_{\mathrm{o}},L)K_{\mathrm{F-Gin}}(t,L) \\ &\sim L\,\kappa_{\mathrm{TI-Gin}}\left(\frac{L}{L_{\mathrm{TI}}^*}\right)\left[\kappa_{\mathrm{F-Gin}}\left(\frac{L}{L_{\mathrm{F}}^*}\right)+t\right]\ , \end{aligned} \quad (12)$$

and sees that the emerging scaling form depends on the ratio between the relevant length scales, namely L_{F}^* and L_{TI}^*. For instance, if $L_{\mathrm{TI}}^* \ll L_{\mathrm{F}}^*$ at large t, the appropriate scaling limit has $x = L/L_{\mathrm{TI}}^*$ fixed, giving the scaling form

$$\kappa^{(\mathrm{TI})}_{\mathrm{TIF-MBQC}}(x) := \lim_{\substack{L,t\to\infty \\ x=L/L_{\mathrm{TI}}^*}} \frac{K_{\mathrm{TIF-Gin}}}{tL} = \kappa_{\mathrm{TI-Gin}}(x) \quad (13)$$

On the contrary, if $L_{\mathrm{F}}^* \ll L_{\mathrm{TI}}^*$ at large t, the appropriate scaling limit has $x = L/L_{\mathrm{F}}^*$ fixed leading to

$$\kappa^{(\mathrm{F})}_{\mathrm{TIF-MBQC}}(x) := \lim_{\substack{L,t\to\infty \\ x=L/L_{\mathrm{F}}^*}} \frac{K_{\mathrm{TIF-MBQC}}}{L} - t = \kappa_{\mathrm{F-Gin}}(x) \quad (14)$$

To test this, in Fig. 2e, we simulate the TI Floquet brick wall model as a representative example, and show that an excellent fit can be obtained using Eq. (12), with L_{F}^* and L_{TI}^* as fitting parameters in Fig. 2f. While we cannot determine the large-t behaviour of L_{TI}^* L_{F}^* from the finite size data, we can extrapolate that $L_{\mathrm{TI}}^* \ll L_{\mathrm{F}}^*$ for this model, and obtain a consistent scaling collapse of (13) in [40].

Discussion. The emergence of universal Ginibre behaviour complements the known emergence of Gaussian unitary ensemble in such systems, and opens up a new avenue to characterize quantum chaos. We emphasize that the emergence of GinUE is a *many-body* quantum phenomenon: Firstly, the construction of spacetime duality requires spatial structure. Secondly, the crossover between linear ramp to exponential behaviours around L_{Th} (or t_{Th}) and the scaling collapse in the scaling limit is a manifestation of *many-body* quantum effect — the (connected) SFF of Gaussian and Circular ensembles have no exponential regime at all.

Acknowledgements. We thank Vir Bulchandani, Soonwon Choi, Giorgio Cipolloni, Ceren Dağ, Michael Gullans, Jonah Kudler-Flam, Igor Klebanov, Daniel Mark, Simeon Mistakidis, Adam Nahum, Vladimir Narovlansky, Hossein Sadeghpour, Grace Sommers and Tianci Zhou for feedback and discussions. AC and ADL warmly thank John Chalker for his guidance in related projects. DAH is supported in part by NSF QLCI grant OMA-2120757. AC is supported by fellowships from the Croucher foundation and the PCTS at Princeton University. The numerics were performed using Princeton Research Computing resources at Princeton University. ADL acknowledges support by the ANR JCJC grant ANR-21-CE47-0003 (TamEnt).

[1] M. L. Mehta, Random Matrices (Academic Press, 2004).
[2] F. Haake, Quantum Signatures of Chaos (Springer, 2010).
[3] O. Bohigas, M.-J. Giannoni, and C. Schmit, Characterization of chaotic quantum spectra and universality of level fluctuation laws, Physical Review Letters **52**, 1 (1984).
[4] A. L. Altshuler and B. I. Shklovskii, Repulsion of energy levels and conductivity of small metal samples, JETP **64**, 127 (1986).
[5] A. Nahum, J. Ruhman, S. Vijay, and J. Haah, Quantum entanglement growth under random unitary dynamics, Phys. Rev. X **7**, 031016 (2017).
[6] T. Zhou and A. Nahum, Emergent statistical mechanics of entanglement in random unitary circuits, Phys. Rev. B **99**, 174205 (2019).
[7] Y. Li, X. Chen, and M. P. A. Fisher, Quantum zeno effect and the many-body entanglement transition, Phys. Rev. B **98**, 205136 (2018).
[8] B. Skinner, J. Ruhman, and A. Nahum, Measurement-induced phase transitions in the dynamics of entanglement, Phys. Rev. X **9**, 031009 (2019).
[9] Y. Li, X. Chen, and M. P. A. Fisher, Measurement-driven entanglement transition in hybrid quantum circuits, Phys. Rev. B **100**, 134306 (2019).
[10] A. Chan, R. M. Nandkishore, M. Pretko, and G. Smith, Unitary-projective entanglement dynamics, Phys. Rev. B **99**, 224307 (2019).
[11] M. J. Gullans and D. A. Huse, Dynamical purification phase transition induced by quantum measurements, Phys. Rev. X **10**, 041020 (2020).
[12] Y. Bao, S. Choi, and E. Altman, Theory of the phase transition in random unitary circuits with measurements, Phys. Rev. B **101**, 104301 (2020).
[13] C.-M. Jian, Y.-Z. You, R. Vasseur, and A. W. W. Ludwig, Measurement-induced criticality in random quantum circuits, Phys. Rev. B **101**, 104302 (2020).
[14] A. Zabalo, M. J. Gullans, J. H. Wilson, S. Gopalakrishnan, D. A. Huse, and J. H. Pixley, Critical properties of the measurement-induced transition in random quantum circuits, Phys. Rev. B **101**, 060301 (2020).
[15] A. Nahum, S. Vijay, and J. Haah, Operator spreading in random unitary circuits, Phys. Rev. X **8**, 021014 (2018).

[16] C. W. von Keyserlingk, T. Rakovszky, F. Pollmann, and S. L. Sondhi, Operator hydrodynamics, otocs, and entanglement growth in systems without conservation laws, Phys. Rev. X **8**, 021013 (2018).

[17] T. Rakovszky, F. Pollmann, and C. W. von Keyserlingk, Diffusive hydrodynamics of out-of-time-ordered correlators with charge conservation, Phys. Rev. X **8**, 031058 (2018).

[18] V. Khemani, A. Vishwanath, and D. A. Huse, Operator spreading and the emergence of dissipation in unitary dynamics with conservation laws, ArXiv e-prints (2017), arXiv:1710.09835 [cond-mat.stat-mech].

[19] A. Chan, A. De Luca, and J. T. Chalker, Solution of a minimal model for many-body quantum chaos, Phys. Rev. X **8**, 041019 (2018).

[20] A. Chan, A. De Luca, and J. T. Chalker, Spectral statistics in spatially extended chaotic quantum many-body systems, Phys. Rev. Lett. **121**, 060601 (2018).

[21] P. Kos, M. Ljubotina, and T. Prosen, Many-body quantum chaos: The first analytic connection to random matrix theory, ArXiv e-prints (2017), arXiv:1712.02665 [nlin.CD].

[22] B. Bertini, P. Kos, and T. Prosen, Exact spectral form factor in a minimal model of many-body quantum chaos, Physical review letters **121**, 264101 (2018).

[23] A. Chan, S. Shivam, D. A. Huse, and A. De Luca, Many-body quantum chaos and space-time translational invariance, arXiv preprint arXiv:2109.04475 (2021).

[24] A. Chan, A. De Luca, and J. T. Chalker, Eigenstate correlations, thermalization, and the butterfly effect, Phys. Rev. Lett. **122**, 220601 (2019).

[25] A. J. Friedman, A. Chan, A. De Luca, and J. T. Chalker, Spectral statistics and many-body quantum chaos with conserved charge, Phys. Rev. Lett. **123**, 210603 (2019).

[26] A. Chan, A. De Luca, and J. T. Chalker, Spectral lyapunov exponents in chaotic and localized many-body quantum systems, Phys. Rev. Research **3**, 023118 (2021).

[27] S. Moudgalya, A. Prem, D. A. Huse, and A. Chan, Spectral statistics in constrained many-body quantum chaotic systems, Phys. Rev. Research **3**, 023176 (2021).

[28] H. Gharibyan, M. Hanada, S. H. Shenker, and M. Tezuka, Onset of random matrix behavior in scrambling systems, Journal of High Energy Physics **2018**, 10.1007/jhep07(2018)124 (2018).

[29] P. Saad, S. H. Shenker, and D. Stanford, A semiclassical ramp in syk and in gravity (2019), arXiv:1806.06840 [hep-th].

[30] M. Akila, D. Waltner, B. Gutkin, and T. Guhr, Particle-time duality in the kicked ising spin chain, Journal of Physics A: Mathematical and Theoretical **49**, 375101 (2016).

[31] B. Bertini, P. Kos, and T. Prosen, Random matrix spectral form factor of dual-unitary quantum circuits (2021), arXiv:2012.12254 [math-ph].

[32] N. Hahn and D. Waltner, Dual approach to the spectral form factor, Acta Physica Polonica A **136**, 841 (2019).

[33] P. Braun, D. Waltner, M. Akila, B. Gutkin, and T. Guhr, Transition from quantum chaos to localization in spin chains, Phys. Rev. E **101**, 052201 (2020).

[34] A. Lerose, M. Sonner, and D. A. Abanin, Influence matrix approach to many-body floquet dynamics (2020), arXiv:2009.10105 [cond-mat.str-el].

[35] M. Ippoliti and V. Khemani, Postselection-free entanglement dynamics via spacetime duality, Phys. Rev. Lett. **126**, 060501 (2021).

[36] M. Ippoliti, T. Rakovszky, and V. Khemani, Fractal, logarithmic and volume-law entangled non-thermal steady states via spacetime duality (2021), arXiv:2103.06873 [quant-ph].

[37] T.-C. Lu and T. Grover, Entanglement transitions via space-time rotation of quantum circuits (2021), arXiv:2103.06356 [quant-ph].

[38] T.-G. Zhou, Y.-N. Zhou, P. Zhang, and H. Zhai, Space-time duality between quantum chaos and non-hermitian boundary effect (2021), arXiv:2107.01901 [cond-mat.str-el].

[39] The non-Hermitian GinUE RMT universality class is also known as non-Hermitian class A [65]. The label “U” in GinUE indicates that the distribution is invariant under unitary conjugation, although the Ginibre matrices themselves are non-unitary.

[40] See supplementary material at [url] for definitions of MBQC and Ginibre models, SFF regime diagrams, spectral properties and correlation of dual spectra, SFF analytical computations of the Ginibre ensemble and its variants, and further numerical results.

[41] A. Flack, B. Bertini, and T. Prosen, Statistics of the spectral form factor in the self-dual kicked ising model (2020), arXiv:2009.03199 [nlin.CD].

[42] J. S. Cotler, G. Gur-Ari, M. Hanada, J. Polchinski, P. Saad, S. H. Shenker, D. Stanford, A. Streicher, and M. Tezuka, Black holes and random matrices, Journal of High Energy Physics **2017**, 10.1007/jhep05(2017)118 (2017).

[43] J. Cotler, N. Hunter-Jones, J. Liu, and B. Yoshida, Chaos, complexity, and random matrices, Journal of High Energy Physics **2017**, 48 (2017).

[44] A. Altland and D. Bagrets, Quantum ergodicity in the syk model, Nuclear Physics B **930**, 45 (2018).

[45] S. J. Garratt and J. T. Chalker, Local pairing of feynman histories in many-body floquet models, Phys. Rev. X **11**, 021051 (2021).

[46] S. J. Garratt and J. T. Chalker, Many-body delocalization as symmetry breaking, Phys. Rev. Lett. **127**, 026802 (2021).

[47] J. Li, T. c. v. Prosen, and A. Chan, Spectral statistics of non-hermitian matrices and dissipative quantum chaos, Phys. Rev. Lett. **127**, 170602 (2021).

[48] D. V. Vasilyev, A. Grankin, M. A. Baranov, L. M. Sieberer, and P. Zoller, Monitoring quantum simulators via quantum nondemolition couplings to atomic clock qubits, PRX Quantum **1**, 020302 (2020).

[49] L. K. Joshi, A. Elben, A. Vikram, B. Vermersch, V. Galitski, and P. Zoller, Probing many-body quantum chaos with quantum simulators (2021), arXiv:2106.15530 [quant-ph].

[50] A. Prakash, J. H. Pixley, and M. Kulkarni, Universal spectral form factor for many-body localization, Phys. Rev. Research **3**, L012019 (2021).

[51] M. Winer, S.-K. Jian, and B. Swingle, Exponential ramp in the quadratic sachdev-ye-kitaev model, Phys. Rev. Lett. **125**, 250602 (2020).

[52] K. Wittmann W., E. R. Castro, A. Foerster, and L. F. Santos, Interacting bosons in a triple well: Preface of many-body quantum chaos, Phys. Rev. E **105**, 034204 (2022).

[53] Y. Liao, A. Vikram, and V. Galitski, Many-body level statistics of single-particle quantum chaos, Phys. Rev.

Lett. **125**, 250601 (2020).

[54] Y. Liao and V. Galitski, Emergence of many-body quantum chaos via spontaneous breaking of unitarity, Physical Review B **105**, L140202 (2022).

[55] J. Cornelius, Z. Xu, A. Saxena, A. Chenu, and A. del Campo, Spectral filtering induced by non-hermitian evolution with balanced gain and loss: Enhancing quantum chaos, Phys. Rev. Lett. **128**, 190402 (2022).

[56] The dimensions of the Hilbert space that the operator acts on in general depends on the model. For the brickwall model in Fig. 1 (where $t = 4, L = 4$), it is q^{2t} for the time transfer matrix and q^{2L} for the space transfer matrix, q being the on-site dimension. On the other hand for the random phase model and the kicked Ising model, it is q^t for the time transfer matrix and q^L for the space transfer matrix.

[57] M. Akila, D. Waltner, B. Gutkin, and T. Guhr, Particle-time duality in the kicked ising spin chain, Journal of Physics A: Mathematical and Theoretical **49**, 375101 (2016).

[58] S. Gopalakrishnan and A. Lamacraft, Unitary circuits of finite depth and infinite width from quantum channels, Phys. Rev. B **100**, 064309 (2019).

[59] A. Lerose, M. Sonner, and D. A. Abanin, Influence matrix approach to many-body floquet dynamics, Phys. Rev. X **11**, 021040 (2021).

[60] J. Li, S. Yan, T. Prosen, and A. Chan, in preparation.

[61] At early time $|\tau| \ll \Delta^{-1}$, DSFF dips from $K(0, \theta) = N^2$ with a form described by the non-universal disconnected DSFF, $\left|\left\langle \sum_n e^{ix_n t + iy_n s} \right\rangle\right|^2$, discussed in [47], but excluded in Eq. (4) for brevity.

[62] L. Sá, P. Ribeiro, and T. c. v. Prosen, Complex spacing ratios: A signature of dissipative quantum chaos, Phys. Rev. X **10**, 021019 (2020).

[63] J. Ginibre, Statistical ensembles of complex, quaternion, and real matrices, Journal of Mathematical Physics **6**, 440 (1965), https://doi.org/10.1063/1.1704292.

[64] M. V. Berry, Semiclassical theory of spectral rigidity, Proceedings of the Royal Society of London A: Mathematical, Physical and Engineering Sciences **400**, 229 (1985).

[65] R. Hamazaki, K. Kawabata, N. Kura, and M. Ueda, Universality classes of non-hermitian random matrices, Phys. Rev. Research **2**, 023286 (2020), arXiv: 1904.13082.